Batys, Piotr; Kivistö, Samu; Lalwani, Suvesh Manoj; Lutkenhaus, Jodie L.; Sammalkorpi, Maria

Comparing water-mediated hydrogen-bonding in different polyelectrolyte complexes

Published in:
Soft Matter

DOI:
10.1039/c9sm01193e

Published: 09/10/2019

Document Version
Peer-reviewed accepted author manuscript, also known as Final accepted manuscript or Post-print

Published under the following license:
Unspecified

Please cite the original version:
Batys, P., Kivistö, S., Lalwani, S. M., Lutkenhaus, J. L., & Sammalkorpi, M. (2019). Comparing water-mediated hydrogen-bonding in different polyelectrolyte complexes. *Soft Matter*, *15*(39), 7823-7831. https://doi.org/10.1039/c9sm01193e

Comparing Water-Mediated Hydrogen-Bonding in Different Polyelectrolyte Complexes

Piotr Batys, [‖]* *Samu Kivistö,* [§,⊥] *Suvesh Manoj Lalwani,* [†] *Jodie L. Lutkenhaus,* [†,‡] *and Maria Sammalkorpi* [§,⊥]

[‖] Jerzy Haber Institute of Catalysis and Surface Chemistry, Polish Academy of Sciences, Niezapominajek 8, PL-30239 Krakow, Poland

[§] Department of Chemistry and Materials Science, [⊥]Department of Bioproducts and Biosystems, School of Chemical Engineering, Aalto University, P.O. Box 16100, FI-00076 Aalto, Finland

[†]Artie McFerrin Department of Chemical Engineering and [‡]Department of Materials Science and Engineering, Texas A&M University, College Station, Texas 77843, United States

Corresponding author:
ncbatys@cyf-kr.edu.pl

For Table of Contents use only:

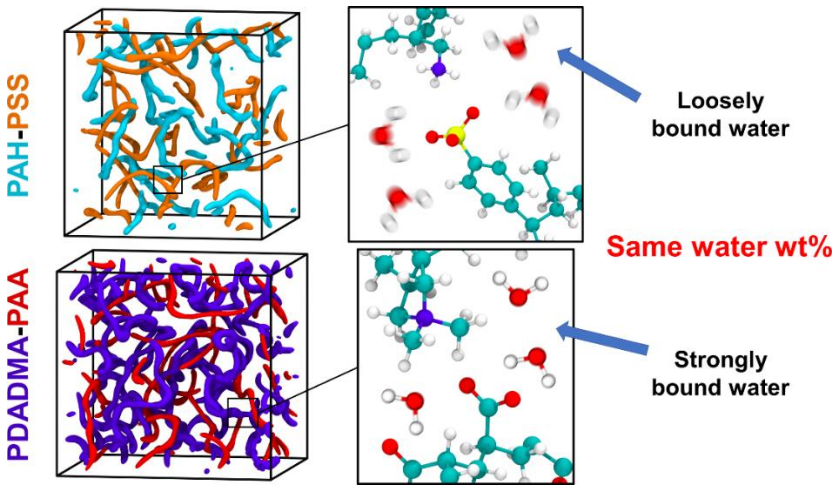

ABSTRACT

All-atom molecular dynamics simulations are used to investigate the polyelectrolyte-specific influence of hydration and temperature on water diffusion in hydrated polyelectrolyte complexes (PECs). Two model PECs were compared: poly(allylamine hydrochloride) (PAH) - poly(sodium 4-styrenesulfonate) (PSS) and poly(diallyldimethylammonium) (PDADMA) - poly(acrylic acid) (PAA). The findings show that the strength of the hydrogen bonding polyelectrolyte-water interaction has enormous influence on the water mobility, which has implications for PEC structure and properties. A 10-fold difference in the average water diffusion coefficient between PAH-PSS and PDADMA-PAA PECs at the same hydration level is observed. The vast majority of the water molecules hydrating the PDADMA-PAA PECs, for hydrations in the range of 26 wt% - 38 wt%, are effectively immobilized, whereas for PAH-PSS PECs the amount of immobilized water decreases with hydration. This points to the polyelectrolyte-specific character of the PE-water hydrogen bonding relationship with temperature. PAA-water hydrogen bonds are found to be significantly less sensitive to temperature than for PSS-water. The polyelectrolyte-water interactions, investigated via radial distribution function, hydrogen bond distance and angle distributions, are connected with resulting structure of the PECs. The PDADMA-PAA and PAH-PSS PECs are prepared experimentally and the states of water at different hydration levels is determined using differential scanning calorimetry (DSC). Experiments confirm the differences between PDADMA-PAA and PAH-PSS PECs observed in the theoretical modelling. The results suggest that the initial predictions of the PEC's bonding with water can be based on simple molecular-level considerations.

INTRODUCTION

Self-assembly of polyelectrolytes (PEs) bearing opposite charges leads to the formation of polyelectrolyte complexes (PECs). The broad interest in PECs is associated with the ease of their preparation and potential to tune their properties. The growing variety of available PEs with varying bonding strength[1] allows the control of the synthesized PECs. Additionally, their properties can be further tuned via formation conditions[2–4] or post-treatment modification.[5–10] As many important biological macromolecules, such as DNA, RNA, polypeptides or polysaccharides are highly charged PEs, PECs are also promising materials in the fields of biotechnology and medicine.[11]

The role of water in hydrated PECs is of great importance for their thermal and mechanical properties.[12,13] Water contributes to PEC plasticization by lubricating the PE chains (increasing PE sliding) and by simultaneously enhancing the free volume. Additionally, water acts as a nontraditional plasticizer by partially screening the electrostatic interactions between PEs. All of these effects facilitate polymer chain motion.[6,14–16] It is worth mentioning that organic alcohol solvents such as n-butanol, ethylene glycol, or 1-propanol have no plasticization effect on PECs.[17] The rheological behavior of PECs can be controlled by water, temperature, salt or pH, and various combinations of the superposition principle can be applied to the response.[6,18–20] Interestingly, the mobility of water molecules[21] and PEs[6] in PECs are similarly affected by the changes in the temperature and hydration.

Based on its melting temperature T_m, measured using differential scanning calorimetry (DSC), water within PECs can be divided into three different states: 1) non-freezing bound water, W_{nf} (no detectable T_m); 2) freezing bound water, W_{fb} (T_m below 273 K); and 3) freezing free water, W_{ff} (T_m close to 273 K).[21,22] Respectively, the non-freezing or freezing bound water corresponds to water molecules that are tightly or weakly bound to the PEs, respectively. For PDADMA-PSS PECs,[21] as well as for swollen poly(vinyl alcohol),[14] the water content required to observe any freezing water was around 30wt%. However, the chemistry and size of the PE's charged group are expected to strongly influence how the water molecules distribute into different water states within the PEC.

To better understand the previously mentioned PEC properties, molecular-level insight on the origins of both the universal characteristics of PECs and also PE-specific effects are needed. For this, computational methods[23] such as Molecular Dynamics (MD) or Monte Carlo[24–27] methods can be utilized. Coarse-grained MD provides access to PE self-assembly,[28,29] complex coacervation,[30–32] and dynamics in the PECs,[33] while explicit solvent all-atom MD simulation enables investigation of the formation of PE assemblies,[34–36] microscopic structure,[37] intrinsic and extrinsic ion pairing,[6,38] and the dynamics of the water molecules and ions in hydrated PECs.[16,17,38–41] For example, MD simulations accounted for PEC thermal transition by pointing out the importance of PE-water hydrogen bonds,[17,38] and explained the role of water and salt in plasticization.[16] Recently, MD simulations were used for detailed analysis of the water mobility in PDADMA-PSS PECs.[21]

Here, we compare the nature of water in hydrated PAH-PSS and PDADMA-PAA PECs via all-atom detail MD simulations. This enables the assessment of PE chemistry and provides a unique way of understanding their general behavior, such as swelling or decomposition. In contrast, our previous work on hydrated PECs[4,6,16,17,21,38] has not made these comparisons and has largely focused on PDADMA-PSS or PAH-PAA PECs. Specifically, we highlighted the difference in the hydration and temperature response of the water diffusion coefficients in PAH-PSS and PDADMA-PAA PECs and connected it with the nature of PE-water interactions. The simulations provided detailed information about water organization around the polyelectrolytes in hydrated PECs and enabled assessment of the role of PE-water hydrogen bonding. Finally, the simulations findings were verified using DSC experiments. Major differences in water behavior were found between PAH-PSS and PDADMA-PAA PECs. Connecting the molecular-level information with the resulting PEC structure and properties as a function of PE type, temperature, and hydration is expected to significantly enhance the understanding of PEC materials response and provide valuable insight into designing PEC materials with precisely defined characteristics.

MATERIALS AND METHODS

Experiments

Poly(allylamine hydrochloride) (PAH, Mw = 120,000 – 200,000 g mol^{-1}, 40 wt% in water) was purchased from Polysciences Inc. and Poly(sodium 4-styrenesulfonate) (PSS, Mw = 500,000 g mol^{-1}) from Scientific Polymer Products. Poly(diallyldimethylammonium chloride) (PDADMA, Mw = 200,000 – 350,000 g mol^{-1}, 20 wt% in water) and poly(acrylic acid) (PAA, Mw = 100,000 g mol^{-1}, 35 wt% in water) were purchased from Sigma Aldrich and used as received. We employ here the terms PAH, PSS, PDADMA, and PAA to refer to PEs that are ionized or partially ionized (e.g. PAA actually has some amount of charge and is not existing in its fully acidic form). As the differences resulting from the side group chemistry were the major interest in this work, the effects of chain length and tacticity were not considered. Milli-Q water with 18.2 MΩ-cm resistivity was used for all solutions and 1 M NaOH or 1 M HCl were used for pH adjustment.

The concentrations of PE solutions were 50 mM with respect to polymer repeat unit. In order to obtain PAH-PSS PECs, the pH of PAH and PSS solutions were separately adjusted to 3.5, and 100 mL PAH solution was added quickly into 100 mL PSS solution while stirring. The mixture became cloudy-white as a complex precipitate was formed. For PDADMA-PAA PECs, the pH of PDADMA and PAA solutions were separately adjusted to 9.0, and 100 mL PDADMA solution was added quickly into 100 mL PAA solution while stirring. The mixture turned cloudy, and then a sticky gel-like complex precipitate was formed. The PEC precipitate was collected after centrifugation at 8500 rpm for 10 min. The PECs were first air-dried overnight and then vacuum-dried at 50 ºC for 12 h. Afterward, the PECs were ground into a powder, which was then further vacuum-dried at 50 ºC for 2 d prior to characterization.

The state of water in a hydrated PEC was determined using DSC, as described previously.[21] In brief, the hydrated sample was cooled from 293 K to 223 K at 5 K min^{-1}, kept isothermally, and then

heated back to 293 K at the same rate. All DSC thermograms are shown in "exotherm down" format and correspond to the 2nd heating cycle unless otherwise stated.

The weight fraction of freezing water (W_f) was calculated using the following equation:[22]

$$W_f = \frac{\Delta H_m}{\Delta H_0} \quad (1)$$

where ΔH_m is the enthalpy of melting of the frozen water in the PEC (obtained from integration of the melting endotherm) and ΔH_0 is the enthalpy of melting pure Milli-Q water, which is 329 J g^{-1} as reported previously.[22] Then, freezing water was classified into freezing free water, W_{ff}, or freezing bound water, W_{fb}, based on the melting temperature, T_m, as described before. The mass of non-freezing bound water (W_{nf}) is given by:

$$W_{nf} = W_c - W_f \quad (2)$$

where W_c is the total water content of hydrated PEC.

Molecular Dynamics Simulations

All-atom MD simulations were performed using the Gromacs software, version 5.1.4.[42,43] Two different pairs of PEs have been studied, PAH-PSS and PDADMA-PAA. All the PECs contained 20 polyanion and 20 polycation chains. All the PEs chains were fully charged and consisted of 20 repeat units each. The chemical structures of the investigated PEs, and the simulation snapshots of the single monomers with their hydration shell are presented in **Figure 1**. Four different water concentrations were examined, i.e., 26, 30, 34, and 38 wt%. The detailed compositions of the PECs can be found in Table S1. Due to the differing molar masses of the PEs, a particular hydration (in wt%) leads to a different number of the water molecules per repeat unit for PAH-PSS and PDADMA-PAA at a particular hydration. The effect of this on the presented results is much less than that of the PE chemistry.

The OPLS-aa force field[44] with the ammonium groups extension[45] and the TIP4P explicit water model[46] were used. As empirical water models, including TIP4P, differ in their diffusion coefficient predictions, we assessed the response of pure water system as a function of temperature in Ref.[21], finding the temperature response to be in agreement with experiments. However, the absolute self-diffusion coefficient value is overestimated by the model.[47] The validity of the PE models, and their water interactions, were checked against the radius of gyration.[16] Initial configurations of PECs were generated using PACKMOL,[48] with a protocol established in previous work,[6,21,38] using PE chain conformations extracted from dilute solution, see **Figure 1**. The long-range electrostatics interactions were calculated using the PME method.[49] Van der Waals interactions were described using the Lennard-Jones potential with a 1.0 nm cut-off. In order to use a 2 fs time step, all the bonds in polyelectrolytes and in water molecules were constrained using the LINCS[50] and SETTLE[51] algorithms, respectively. Temperature was controlled, separately for the polyelectrolytes and solvent, via the V-rescale thermostat[52] with a coupling constant $\tau = 0.1$ ps. Periodic boundary conditions were applied in all directions. The Parrinello-Rahman barostat[53] with a coupling constant $\tau_p = 2$ ps was used to maintain pressure at 1 bar. All simulation visualizations were done using the VMD software package.[54]

The detailed steps of obtaining PE assemblies with relatively uniform structure and water distribution are gathered in ESI (Table S2). The protocol follows Ref.[38] Briefly, the initial PE configurations generated via Packmol[48] were solvated with the target amount of water, the system initially pressure-equilibrated at 290 K temperature followed by a 100 ns initial NPT relaxation at an elevated temperature of 370 K. After this, the temperature was brought down to 290 K in 10 ns time. This procedure leads to the configurational energy, density distributions, and box volume (system density) values vs. time plots reaching a plateau. All of these, were used as local equilibration criteria but high density (small box volume) of the resulting PE-water assembly was used for choosing the configurations for the production runs: high, uniform density means the configurations are uniformly

packed and compact. Notably, under low hydration, the PEs easily get pinned to configurations corresponding to artificially low density; no such configurations were accepted as initial configurations for the productions runs. Following this protocol, locally relaxed, relatively uniformly mixed initial configurations were obtained for the production run. In the production run, the temperature was increased from 290 K to 360 K in 5 K steps of 15 ns each for a total simulation duration of 225 ns. The first 1 ns of each step was disregarded in the analysis. The employed timescale is too short to capture polymer chain relaxation and diffusion but water dynamics is captured.[55] All presented results were calculated as an average over simulations corresponding to three different initial configurations.

The diffusion coefficients were calculated using the Einstein relation; the obtained D corresponds to the least squares fitting to the linear section of the mean square displacement (MSD) of the center of mass of the water molecules in the analysis period. The distributions of diffusion coefficients for individual water molecules were determined from separate 20 ps long simulations with an enhanced output frequency of 10 fs, following Ref.[21] The radial distribution function (RDF) between particles of type A and B was defined as follows:

$$\mathrm{RDF} = \frac{1}{\langle \rho_B \rangle_{local}} \frac{1}{N_A} \sum_{i \in A}^{N_A} \sum_{j \in B}^{N_B} \frac{\delta(r_{ij} - r)}{4\pi r^2}, \quad (3)$$

where $\langle \rho_B(r) \rangle$ is the particle density of type B at a distance r around particles A, and $\langle \rho_B \rangle_{local}$ is the particle density of type B averaged over all spheres around particles A with radius $r_{\max}$ (half of the simulation box length). The RDF between the PE and water molecules was calculated as distance (r) distribution between any individual atom position in the molecules. This provided additional information about the orientation of water molecules around PEs.

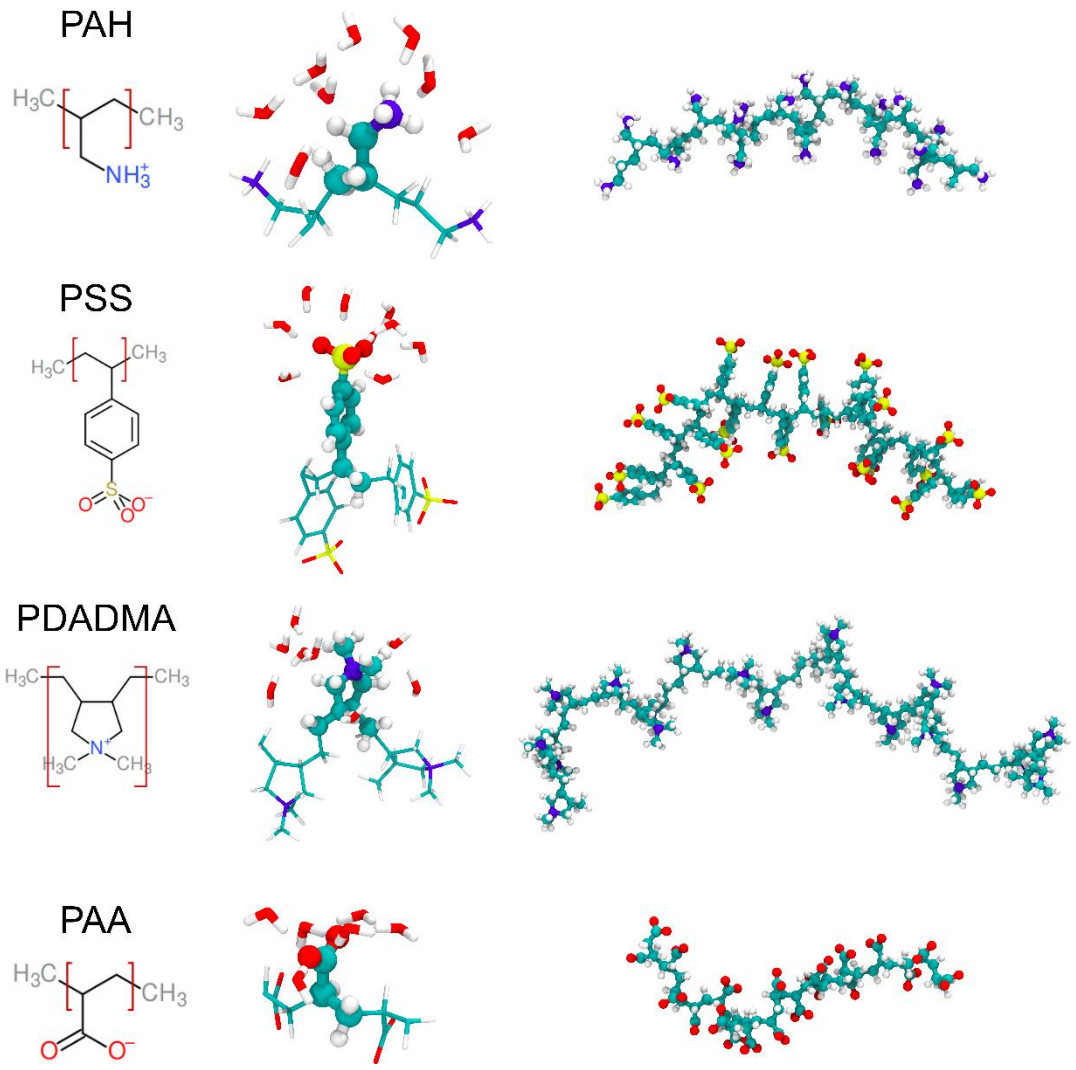

Figure 1. The PE chemical structures (on the left), their single repeat unit surrounded by water molecules (in the middle), and (on the right) the conformation of 20 repeat unit long chains, used for generating the PECs, derived from MD simulations in bulk water.

RESULTS AND DISCUSSION

Water mobility in the PAH-PSS and PDADMA-PAA PECs was investigated by calculating the average diffusion coefficient of water, D, as a function of water wt% and temperature, **Fig. 2**. For clarity, we used a constant y-axis range and plotted ln$D$ vs $1/T$. At equivalent hydration levels, we observed a 10-fold difference in D between the PAH-PSS and PDADMA-PAA PECs, indicating that water within PAH-PSS PECs is much more mobile. The D-value for the PAH-PSS PEC at 26 wt% and 290 K was comparable to D-value for the PDADMA-PAA PEC at 38 wt% and 330 K. Such

discrepancy in water mobility indicates significant differences in the relative PE-water interactions. The character of the temperature dependency (slope on **Fig. 2**) is different for these two PE pairs. The slope for the PAH-PSS PEC seems to be less sensitive to hydration changes, whereas the slope for PDADMA-PAA PEC significantly increases with the water wt%. The exponential relationship between D and T can be described using an Arrhenius-type equation:

$$\ln D = \ln D_0 - \frac{E_a}{k_B}\frac{1}{T}, \quad (4)$$

where the parameter E_a is an activation energy for the diffusion, and D_0 is a diffusion coefficient at $T \to \infty$. A fit of Equation (4) to the data in Fig. 2 yields E_a and D_0 via least-squares fitting, Table 1. The E_a-value represents here the energy required for water molecule migration and disruption of the energy barriers in the PEC network, such as PE-water hydrogen bonds.[38]

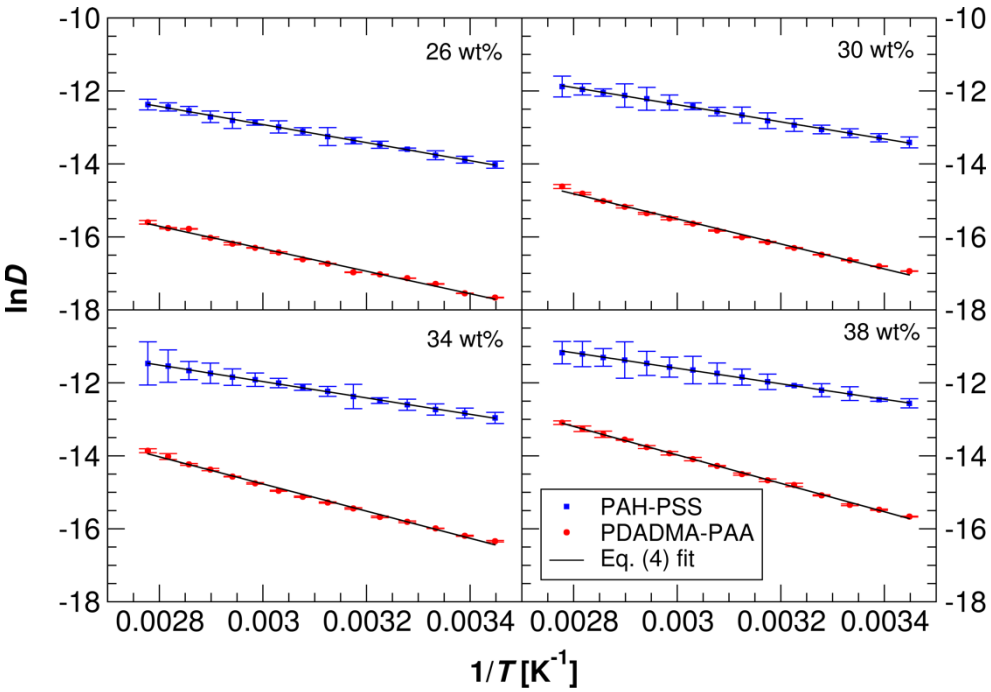

Figure 2. The average diffusion coefficient (D) of water molecules as a function of the temperature in PECs of varying hydration. Lines denote fitting of Equation (4) to the simulated data points. The MSD curves used to calculate D are presented in the ESI, Figure S1.

Table 1. The activation energy E_a and maximal diffusion coefficient D_0 corresponding to the Arrhenius Equation (Equation 4) obtained via least squares fitting to data in Figure 2.

PE pair	Hydration [wt%]	E_a [kJ/mol]	$D_0 \times 10^3$ [cm^2/s]	R^2
PAH-PSS	**26**	20.60 ± 0.03	4.13 ± 0.01	0.9993
	30	19.52 ± 0.03	4.82 ± 0.01	0.9992
	34	18.70 ± 0.02	5.44 ± 0.01	0.9995
	38	17.65 ± 0.03	5.35 ± 0.01	0.9991
PDADMA-PAA	**26**	25.62 ± 0.08	0.84 ± 0.01	0.9968
	30	28.54 ± 0.10	5.48 ± 0.02	0.9968
	34	30.93 ± 0.11	27.0 ± 0.1	0.9977
	38	32.40 ± 0.07	102.0 ± 0.2	0.9992

The data presented in Table 1 show the rather unexpected behavior of E_a with hydration. For PAH-PSS PECs E_a decreases with the hydration, whereas the opposite trend can be observed for PDADMA-PAA PECs. The reason for the opposite trends of E_a versus hydration observed for the two different PECs is not yet completely clear. We speculate that the opposite trends are related to the exceptionally strong affinity of PAA to water in PDADMA-PAA PECs, as opposed to the weaker affinity for PSS. We compared the E_A values with our prior work for PDADMA-PSS PECs,[21] where for similar hydrations the E_A was around 17 - 19 [kJ/mol]. However, the E_A in that work was calculated using only the translational component of the diffusion coefficient, so the values are expected to be slightly underestimated in comparison to the E_A-values in Table 1.

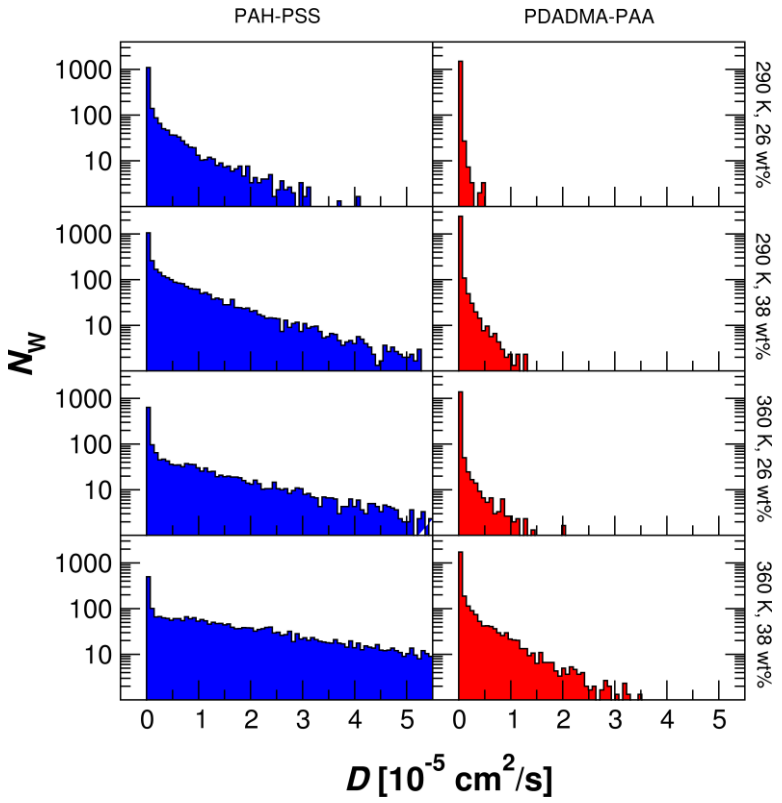

Figure 3. Individual water molecule diffusion coefficients as population frequency histograms for PAH-PSS and PDADMA-PAA PECs at selected water contents and temperatures. The data correspond to the average from three different initial configurations and are calculated over a period of 20 ps. The histograms for a wider range of water contents and temperatures can be found in ESI, Figure S2.

The population frequency histograms presented on **Figure 3** show the distribution of individual water molecules' *D* values in the PECs at different temperature and hydration levels. The data enables distinction between the bound and non-bound water states.[21] Huge differences can be observed between the distributions of the *D* values for water molecules in PAH-PSS vs. PDADMA-PAA PECs. The PDADMA-PAA PECs appear to have a much tighter distribution; the fraction of mobile water is much lower in PDADMA-PAA PECs than in PAH-PSS PECs. The distribution profile for PDADMA-PAA with 38 wt% of water at 360 K is similar to PAH-PSS with 26 wt% at 290 K. Interestingly, the first peak, corresponding for strongly bound water, decreases with hydration and temperature for PAH-PSS, while for PDADMA-PAA it is much less affected. However, regardless of the temperature or hydration, a majority of water molecules have a very low *D*. These immobilized water molecules, which constitute most of the water even at elevated hydrations, can be considered as being tightly

bound to the PE.[21]

Hydration and temperature changes lead to very similar distribution profiles. Previously, this has been found for PDADMA-PSS systems,[21] but observing the effect for the PECs studied here suggests that this could be a more generalized phenomena. The distribution of individual water molecule *D* values for PDADMA-PSS[21] is very similar as for PAH-PSS, **Figure 3**.

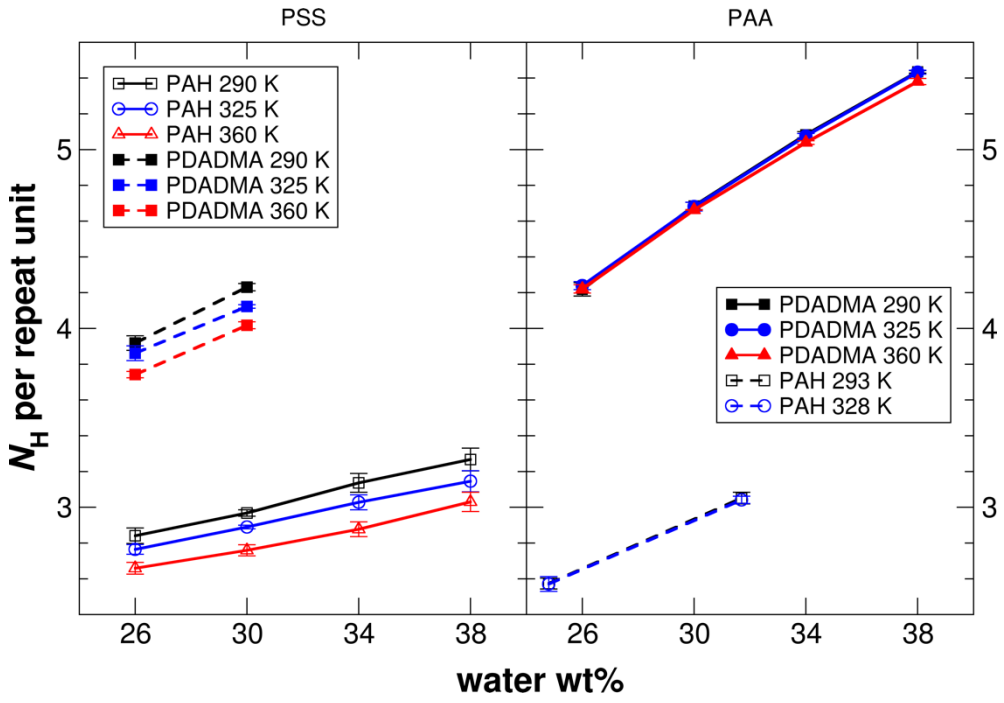

Figure 4. The number of H-bonds between the polyanion and water (N_H) per single polyanion repeat unit as a function of the PEC type, temperature, and water wt%. Results for PDADMA-PSS and PAH-PAA PECs were calculated using previously studied systems in Ref.[21] and Ref.[6], respectively.

To better understand the differences in the water mobility we analyzed the differences in the PE-water interactions. In **Figure 4**, we have presented the average number of polyanion-water hydrogen bonds (N_H) per single polyanion charge group as a function of the temperature and hydration. For a comparison, we have also calculated this for previously studied PDADMA-PSS[21] and PAH-PAA[6] systems. All of the presented results are for fully charged PEs and without counterions, except the PDADMA-PSS PECs, where a small amount of Cl^- ions were added to neutralize the system. Interestingly, the findings suggest that the number of H-bonds between the polyanion and water is

dictated by the polycation type, and less influenced by the polyanion itself. For PECs containing PAH, the number of polyanion-water H-bonds does not appear to be polyanion-sensitive. In the case of PDADMA, the number of the PAA-water H-bonds is higher than that of PSS-water; this could be related to the higher affinity of water for PAA. In PECs containing PDADMA, the number of polyanion-water H-bonds is significantly higher than in the PECs containing PAH. This surprising behavior can be explained by the differences between PAH and PDADMA in ion-pairing strength;[1,56] PDADMA hydrogen bonds with water more weakly than PAH, which allows polyanions to form more H-bonds with water (in the case of PDADMA). PAA's higher affinity to water seems to be disactivated in PAH-PAA PECs due to the strong polyanion-polycation interactions.

Figure S3 presents values of N_H, which are normalized by the number of water molecules in the system (N_W). The N_H/N_W ratio for the PDADMA-PAA PEC is roughly twice as that for the PAH-PSS PEC at a given water wt%. For the PDADMA-PAA PEC with 26 wt% water, the N_H/N_W ratio exceeds one, which means that there are more PAA-water hydrogen bonds than water molecules in the system. Additionally, one can observe that in case of the PDADMA-PAA PEC the effect of temperature is negligible, which results from the strong interaction strength between PAA and water. For the PAH-PSS PEC, the N_H/N_W ratio decreased slightly with the increasing temperature.

We also analyzed the H-bond distance and angle distribution, which are related to the H-bond strength,[57] **Figure S4**. The average length of the PAA-water H-bond in PDADMA-PAA was slightly shorter than the PSS-water H-bond in PAH-PSS. Also, the angle distribution was narrower and shifted towards lower angles in the case of PAA-water H-bonds. Both, the distance and the angle distributions confirm that the PAA-water H-bond in PDADMA-PAA is stronger than the PSS-water H-bond in PAH-PSS PECs. For both PAA-water and PSS-water H-bonds, the influence of temperature is significant, while the effect of hydration is much less pronounced.

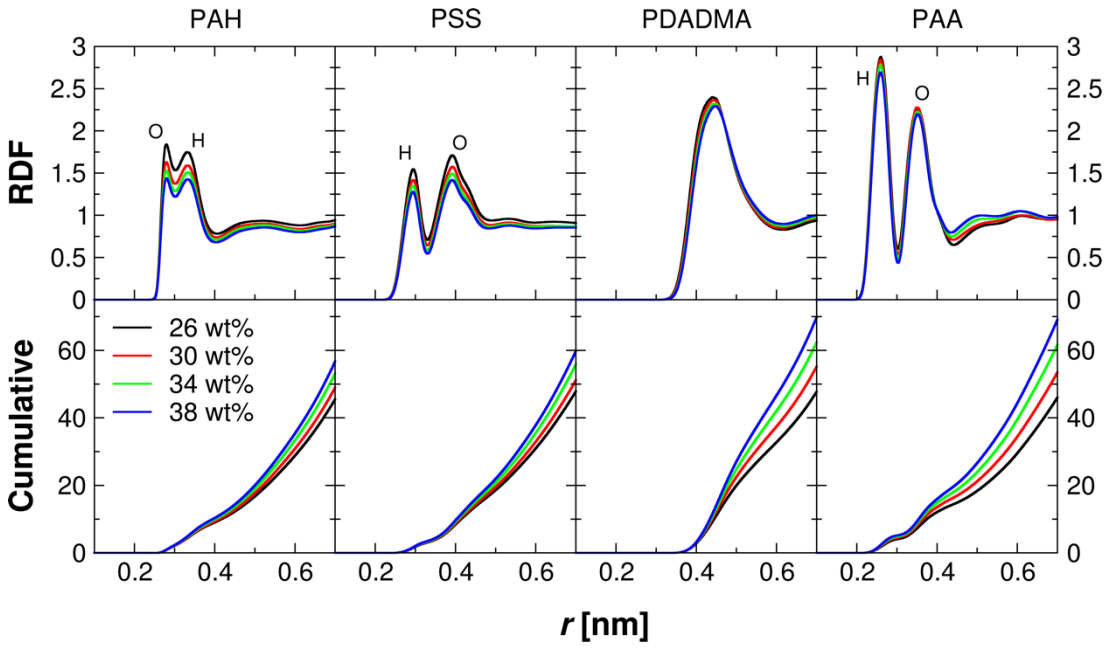

Figure 5. The radial distribution function RDF and cumulative number of water molecules around PEs in the investigated PECs at a different hydration and $T = 290$ [K].

To gain more insight into the water distribution and orientation around specific PEs, we calculated the radial distribution function (RDF) and the cumulative number of water molecules, see **Fig. 5**. Except for PDADMA, which is unable to form H-bonds with water molecules, all of the PEs exhibited two peaks attributed to the H and O atoms in the water molecule. For PSS and PAA, the closest peak corresponds to the H atom and for PAH to the O atom. This indicates the favorable orientation of water molecules for PAH, PSS, and PAA, respectively. The highest value of the RDF and cumulative number of water molecules, as well as the most pronounced peak separation, was observed for PAA, which was in line with the results presented above. The difference in affinity of PEs to form H-bonds with water molecules partially explains why the side group charge density cannot be used on its own for predicting PE bonding strength.[1] Our results suggest the interplay between PE charge density and H-bond affinity. For PAA, which has a high charge density, one can expect strong bonding with oppositely charged PEs, but, on the other hand, the strong affinity to water molecules makes it very weak.[1]

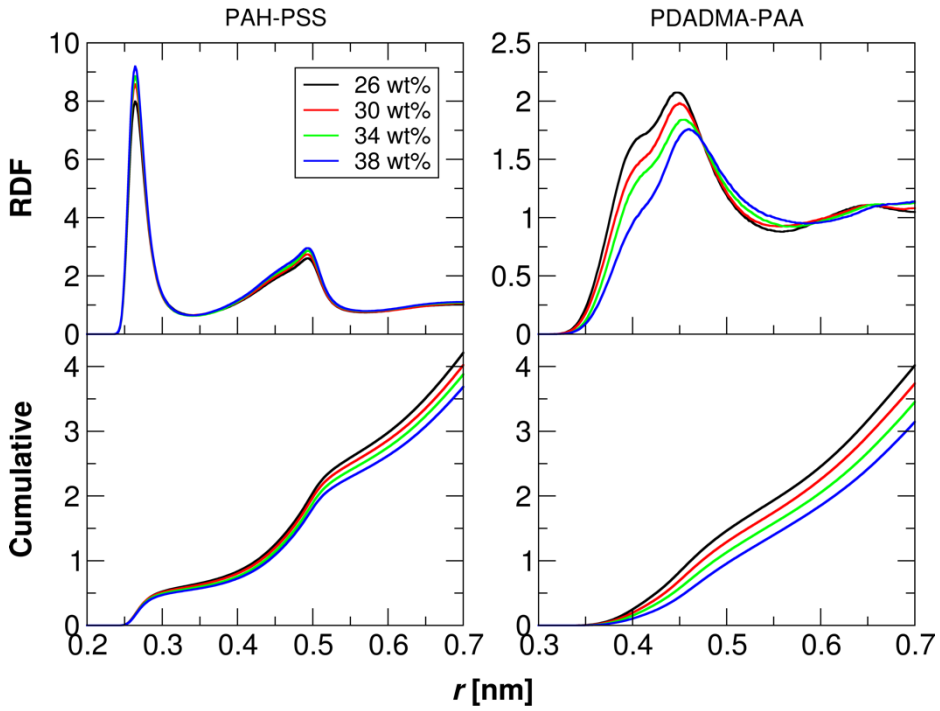

Figure 6. The radial distribution function between PE-PE pairs and its cumulative value at different hydrations and $T = 290$ [K]. The distance r corresponds to the distance between N - O atoms for PAH-PSS and N – O atoms for PDADMA-PAA.

The RDF between the PE-PE charge groups, presented in Fig. 6, provides information on how the PEC structure is affected by the increasing hydration. For both systems, the cumulative number of PE-PE pairs (intrinsic ion pairs) decreased with the increasing water wt%. This might be explained by extra volume introduced by the added water molecules; PEs are, on average, slightly further apart. However, for PAH-PSS the cumulative function at $r = 0.5$ nm is only slightly dependent on hydration, while for PDADMA-PAA the change is more prominent. This is related to the different interaction strengths for PE-PEs and for PE-water. In PDADMA-PAA PECs, the interaction between polymers seems to be weaker than the interaction between PAA and water molecules; accordingly, addition of water slightly decreases the number of intrinsic ion pairs. In fact, it was observed that polar water molecules were strongly oriented near PAA, which may locally compensate or screen PAA's charge. Therefore, water molecules acted here similarly to counterions in other systems,[16,38] and their strong interactions with PAA might be considered as a special type of charge (or dipole) compensation by the high degree of orientation of individual water molecules. In PAH-PSS PECs, on the other hand,

increasing hydration does not significantly influence the number of intrinsic ion pairs. The peak position is roughly the same for the PAH-PSS, but it shifts slightly towards larger distances in case of the PDADMA-PAA PEC. This suggests that PDADMA-PAA electrostatic bonding and PAA-water hydrogen bonding are competitive. The PAH-PAA intrinsic pairs seem to be stronger than PDADMA-PAA, which is in agreement with their experimentally determined ion-pair strengths.[1] The PAA-water interaction strength is somewhere in between, as it is strong enough to break PDADMA-PAA intrinsic pairs, but not PAH-PAA. The strong interactions between PAA-water and the breaking of PDADMA-PAA ion pairs is expected to cause significant swelling of the PEC. It is worth noting that in comparison to PAH-PSS multilayers, PDADMA-PAA multilayers exhibit a significantly higher degree of swelling[58] as well as much lower contact angles.[59] The weaker interaction between PDADMA and PAA may also be responsible for the decomposition of PDADMA-PAA multilayers at intermediate salt concentrations,[60] as well as a higher cation uptake as compared to PAH-PSS.[61] The competition between PE-PE and PE-water bonding is strongly PE-specific and seems to be crucial for the resulting PEC properties; MD simulation provides an easy way to estimate the differences in water bonding between PEs.

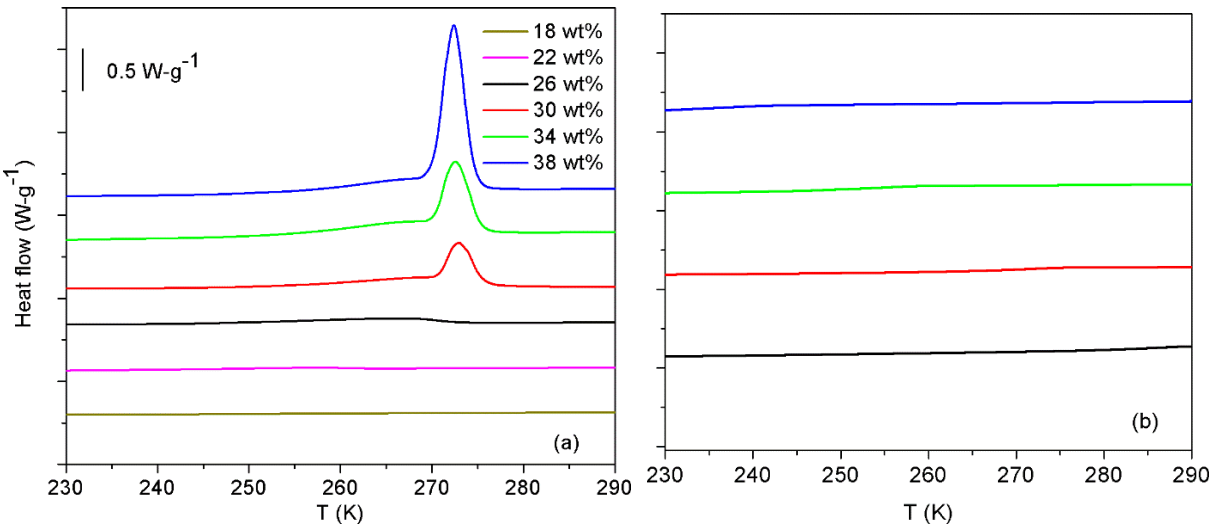

Figure 7. DSC heat flow curves for (a) PAH–PSS and (b) PDADMA-PAA PECs with varying water content. The first heating cycle at 5 K min^{-1} is shown and the data presented correspond to the "exotherm down" format. The scale bar and legend in (a) apply also to panel (b).

To complement the findings from MD simulations, the experimental amount of bound water was determined using DSC of PAH-PSS and PDADMA-PAA PECs. The experimental complexation process exhibited major differences between the two systems, see **Figure S4**. In the case of PAH-PSS, a white precipitate was observed. On the other hand, PDADMA-PAA formed a sticky hydrogel, indicative of PAA's high affinity toward water. Experimentally prepared PECs were isolated, dried, and re-hydrated with a known quantity of water. These hydrated PECs were then quenched to -50 °C and reheated to observe the melting of freezing bound or freezing free water.

DSC thermograms of hydrated PAH-PSS PECs, Figure 7(a), show a narrow melting peak overlapping with a smaller broad melting peak. The broad melting peak is assigned to the melting of water crystals formed from homogenous nucleation, and the narrow melting peak is assigned to those formed from heterogenous nucleation. The narrow peak is close to 273 K at hydration levels greater than 26 wt%, indicating the presence of freezing free water in the system. For lower hydrations, the peak was much broader and the maximum shifted towards lower temperatures, suggesting the presence of small amounts of freezing bound water. From this information, the weight fractions of non-freezing bound water, freezing bound water, and freezing free water were calculated, Table 2. For PAH-PSS PECs, the state of water shifted from non-freezing to freezing bound and then to freezing free (with mixtures thereof) as hydration increased from 18 to 38 wt% water. In contrast, DSC thermograms for hydrated PDADMA-PAA PECs are shown in Figure 7(b). No melting peaks were observed, indicating that only non-freezing bound water was present within the hydration range studied, Table 2.

Table 2. Nonfreezing water W_{nf}, freezing bound water W_{fb}, freezing free water W_f, and melting temperature of water T_m for PAH-PSS and PDADMA-PAA PECs at various hydration levels W_c.

PE pair	**Hydration, W_c [wt%]**	**W_{nf} [wt%]**	**W_{fb} [wt%]**	**W_{ff} [wt%]**	**T_m [K]**

PAH-PSS	**18**	18	n/a	n/a	n/a
	22	21.0 ± 0.5	0.7 ± 0.1	n/a	257.9 ± 1.7
	26	22.8 ± 0.3	3.4 ± 0.3	n/a	265.7 ± 0.3
	30	18.9 ± 0.1	n/a	11.2 ± 0.2	272.2 ± 0.7
	34	17.2 ± 1.0	n/a	16.0 ± 1.5	272.0 ± 0.5
	38	10.8 ± 0.3	n/a	27.1 ± 0.3	272.5 ± 0.1
PDADMA-PAA	**26**	26	n/a	n/a	n/a
	30	30	n/a	n/a	n/a
	34	34	n/a	n/a	n/a
	38	38	n/a	n/a	n/a

n/a indicates that no peak associated with that phenomenon was observed

We next connect experimental observations with those of the MD simulations. The strong interactions present between PAA and water from MD simulations (Figure 5) appear to result in only non-freezing bound water for the experimental PDADMA-PAA system, Table 2. In fact, for PDADMA-PAA PECs, the simulated water diffusion was much lower (Figure 3) than for PAH-PSS PECs, further indicating the extent of bound water. In comparison, PSS-water interactions were much weaker in MD simulations (Figure 5), which resulted in the presence of freezing free water in experimental PAH-PSS PECs at higher hydration, Table 2. This is supported by inspecting water diffusion in PAH-PSS vs PDADMA-PAA systems, Figure 2. PAH-PSS PECs displayed a higher water diffusion coefficient, which can be attributed to the presence of freezing free water. The fraction of non-freezing water decreases with increasing hydration for PAH-PSS PECs. This is probably related to an increase in the water cluster size, what initiates crystallization. In other words, at lower hydration values water molecules form small separated clusters, which then grow with further addition of water. This can also be observed from simulations, Figure 3, in which the number of water molecules that have very low diffusion coefficients decreases significantly with increasing hydration.

To compare with our prior work on the states of water within PDADMA-PSS PECs,[21] the trend

of non-freezing bound water is influenced by the polyanion-polycation and PE-water bonding strength. As shown previously,[21] non-freezing bound water increases with increasing hydration for PDADMA-PSS PECs, which is opposite to the PAH-PSS PEC trend herein. The positive charge on PDADMA's or PAH's nitrogen is affected by the environment, with the former having lower charge density, resulting in weaker interactions with PSS. This leads to a higher fraction of non-freezing bound water (W_{nf}= 29.1%) in PDADMA-PSS[21] when compared with PAH-PSS (W_{nf}=18.9%) at the same hydration (30 wt% water).

CONCLUSIONS

Water bonding and water mobility in hydrated PAH-PSS and PDADMA-PAA assemblies was investigated theoretically using all-atom MD simulations as a function of temperature and hydration. The results showed significant differences between the PAH-PSS and PDADMA-PAA systems. A 10-fold lower diffusion coefficient was found in PDADMA-PAA vs PAH-PSS PECs at the same water wt%. Moreover, the character of the PE-water bonding with temperature was different for these two PECs. The herein observed differences resulted from the various and competing interactions strengths between PE-PE and PE-water molecules. In the case of PAH-PSS PECs, PE-PE ion bonding dominates over PE- water bonding; on the other hand for PDADMA-PAA PECs, the strong PAA-water interactions can compete with PE-PE bonds, causing PEC swelling and a gel-like consistency. We have also compared the hydrogen bonding in the PAH-PSS and PDADMA-PAA PECs with previously studied PAH-PAA[6] and PDADMA-PSS[21] PECs. The findings connect to the more general behavior of PECs and explain the origin of the differences observed in, e.g., swelling behavior,[58] decomposition,[60] counterion uptake[61], and contact angles.[59]

Investigation of the individual water molecule diffusion revealed that in the case of PAH-PSS the fraction of more mobile water is significantly larger than for PDADMA-PAA PECs. Both temperature and hydration increase the water mobility in a very similar manner; however, even for the highest

temperature and hydration investigated, the majority of water molecules were effectively immobilized. This was experimentally supported by the observation of a freezing free water in PAH-PSS PECs and non-freezing bound water in PDAMA/PAA PECs. Our results focus attention on the importance of hydrogen bonding in hydrated PECs and highlight the role of hydration as a control parameter in PEC materials properties.

AUTHOR INFORMATION

Corresponding Author

E-mail: ncbatys@cyf-kr.edu.pl

Notes

There are no conflicts of interest to declare

ACKNOWLEDGEMENT

The authors acknowledge the financial support of the National Science Centre (Poland) under Grant No. 2018/02/X/ST5/02470 (P.B.), Academy of Finland under Grant No. 309324 (M.S.), and National Science Foundation under Grant No. 1609696 (J.L.L). M.S. is grateful for the support by the FinnCERES Materials Bioeconomy Ecosystem. The authors gratefully acknowledge CSC – IT Center for Science, Finland, and RAMI – RawMatTERS Finland Infrastructure for computational resources.

REFERENCES

1 J. Fu, H. M. Fares and J. B. Schlenoff, *Macromolecules*, , DOI:10.1021/acs.macromol.6b02445.

2 Z. Sui, J. A. Jaber and J. B. Schlenoff, *Macromolecules*, 2006, **39**, 8145–8152.

3 Y. Zhang, F. Li, L. D. Valenzuela, M. Sammalkorpi and J. L. Lutkenhaus, *Macromolecules*, 2016, **49**, 7563–7570.

4 Y. Zhang, E. Yildirim, H. S. Antila, L. D. Valenzuela, M. Sammalkorpi and J. L. Lutkenhaus, *Soft Matter*, 2015, **11**, 7392–7401.

5 J. B. Schlenoff, A. H. Rmaile and C. B. Bucur, *J. Am. Chem. Soc.*, 2008, **130**, 13589–13597.

6 P. C. Suarez-Martinez, P. Batys, M. Sammalkorpi and J. L. Lutkenhaus, *Macromolecules*, 2019, **52**, acs.macromol.8b02512.

7 Z. Wang, N. Cai, Q. Dai, C. Li, D. Hou, X. Luo, Y. Xue and F. Yu, *Fibers Polym.*, 2014, **15**, 1406–1413.

8 D. K. Reid, A. Summers, J. O'Neal, A. V. Kavarthapu and J. L. Lutkenhaus, *Macromolecules*, 2016, **49**, 5921–5930.

9 J. T. O'Neal, E. Y. Dai, Y. Zhang, K. B. Clark, K. G. Wilcox, I. M. George, N. E. Ramasamy, D. Enriquez, P. Batys, M. Sammalkorpi and J. L. Lutkenhaus, *Langmuir*, 2017, acs.langmuir.7b02836.

10 C. C. Shiu, S. Wang, C. H. Chang and J. S. Jan, *J. Phys. Chem. B*, 2013, **117**, 10007–10016.

11 M. Rubinstein and G. A. Papoian, *Soft Matter*, 2012, **8**, 9265.

12 H. M. Fares, Q. Wang, M. Yang and J. B. Schlenoff, *Macromolecules*, 2019, **52**, 610–619.

13 R. Koehler, R. Steitz and R. Von Klitzing, *Adv. Colloid Interface Sci.*, 2014, 207, 325–331.

14 R. M. Hodge, T. J. Bastow, G. H. Edward, G. P. Simon and A. J. Hill, *Macromolecules*, 1996, **29**, 8137–8143.

15 H. H. Hariri, A. M. Lehaf and J. B. Schlenoff, *Macromolecules*, 2012, **45**, 9364–9372.

16 R. Zhang, Y. Zhang, H. S. Antila, J. L. Lutkenhaus and M. Sammalkorpi, *J. Phys. Chem. B*, 2017, **121**, 322–333.

17 E. Yildirim, Y. Zhang, J. L. Lutkenhaus and M. Sammalkorpi, *ACS Macro Lett.*, 2015, **4**, 1017–1021.

18 M. Yang, J. Shi and J. B. Schlenoff, *Macromolecules*, 2019, **52**, 1930–1941.

19 R. F. Shamoun, H. H. Hariri, R. A. Ghostine and J. B. Schlenoff, *Macromolecules*, 2012, **45**,

9759–9767.

20 M. Tekaat, D. Bütergerds, M. Schönhoff, A. Fery and C. Cramer, *Phys. Chem. Chem. Phys.*, 2015, **17**, 22552–22556.

21 P. Batys, Y. Zhang, J. L. Lutkenhaus and M. Sammalkorpi, *Macromolecules*, 2018, **51**, 8268–8277.

22 J. Ostrowska-Czubenko, M. Pierõg and M. Gierszewska-Druzyńska, *J. Appl. Polym. Sci.*, 2013, **130**, 1707–1715.

23 T. E. Gartner and A. Jayaraman, *Macromolecules*, 2019, 52, 755–786.

24 J. Jeon and A. V. Dobrynin, *Phys. Rev. E*, 2003, **67**, 061803.

25 C. F. F. Narambuena, E. P. M. P. M. Leiva, M. Chávez-Páez and E. Pérez, *Polymer (Guildf).*, 2010, **51**, 3293–3302.

26 J. S. Kłos and J.-U. Sommer, *J. Chem. Phys.*, 2011, **134**, 204902.

27 Y. Hayashi, M. Ullner and P. Linse, *J. Phys. Chem. B*, 2003, **107**, 8198–8207.

28 F. Jiménez-Ángeles, H.-K. Kwon, K. Sadman, T. Wu, K. R. Shull and M. Olvera de la Cruz, *ACS Cent. Sci.*, 2019, **5**, 688–699.

29 P. A. Patel, J. Jeon, P. T. Mather and A. V. Dobrynin, *Langmuir*, 2006, **22**, 9994–10002.

30 C. E. Sing, *Adv. Colloid Interface Sci.*, 2017, 239, 2–16.

31 L. W. Chang, T. K. Lytle, M. Radhakrishna, J. J. Madinya, J. Vélez, C. E. Sing and S. L. Perry, *Nat. Commun.*, 2017, **8**, 1273.

32 M. Radhakrishna, K. Basu, Y. Liu, R. Shamsi, S. L. Perry and C. E. Sing, *Macromolecules*, 2017, **50**, 3030–3037.

33 M. Vögele, C. Holm and J. Smiatek, *J. Chem. Phys.*, 2015, **143**, 243151.

34 J. Jeon and A. V. Dobrynin, *J. Phys. Chem. B*, 2006, **110**, 24652–24665.

35 A. P. Patel, J. Jeon, P. T. Mather and A. V. Dobrynin, *Langmuir*, 2006, **22**, 9994–10002.

36 N. Hoda and R. G. Larson, *Macromolecules*, 2009, **42**, 8851–8863.

37 D. Diddens, J. Baschnagel and A. Johner, *ACS Macro Lett.*, 2019, **8**, 123–127.

38 Y. Zhang, P. Batys, J. T. O'Neal, F. Li, M. Sammalkorpi, J. L. J. L. Lutkenhaus, J. T. J. T. O'Neal, F. Li, M. Sammalkorpi and J. L. J. L. Lutkenhaus, *ACS Cent. Sci.*, 2018, **4**, 638–644.

39 H. S. Antila, M. Härkönen and M. Sammalkorpi, *Phys. Chem. Chem. Phys.*, 2015, **17**, 5279–5289.

40 H. S. Antila and M. Sammalkorpi, *J. Phys. Chem. B*, 2014, **118**, 3226–3234.

41 B. Qiao, J. J. Cerdà and C. Holm, *Macromolecules*, 2010, **43**, 7828–7838.

42 E. Lindahl, B. Hess and D. van der Spoel, *J. Mol. Model.*, 2001, 7, 306–317.

43 H. J. C. Berendsen, D. van der Spoel and R. van Drunen, *Comput. Phys. Commun.*, 1995, **91**, 43–56.

44 M. J. Robertson, J. Tirado-Rives and W. L. Jorgensen, *J. Chem. Theory Comput.*, 2015, **11**, 3499–3509.

45 J. Gao and W. L. Jorgensen, *J. Phys. Chem.*, 1986, **90**, 2174–2182.

46 W. L. Jorgensen and J. D. Madura, *Mol. Phys.*, 1985, **56**, 1381–1392.

47 M. W. Mahoney and W. L. Jorgensen, *J. Chem. Phys.*, 2001, **114**, 363–366.

48 L. Martinez, R. Andrade, E. G. Birgin and J. M. Martínez, *J. Comput. Chem.*, 2009, **30**, 2157–2164.

49 U. Essmann, L. Perera, M. L. Berkowitz, T. Darden, H. Lee and L. G. Pedersen, *J. Chem. Phys.*, 1995, **103**, 8577–8593.

50 B. Hess, H. Bekker, H. J. C. Berendsen and J. G. E. M. Fraaije, *J. Comput. Chem.*, 1997, **18**, 1463–1472.

51 S. Miyamoto and P. A. Kollman, *J. Comput. Chem.*, 1992, **13**, 952–962.

52 G. Bussi, D. Donadio and M. Parrinello, *J. Chem. Phys.*, , DOI:10.1063/1.2408420.

53 M. Parrinello, *J. Appl. Phys.*, 1981, **52**, 7182.

54 W. Humphrey, A. Dalke and K. Schulten, *J. Mol. Graph.*, 1996, **14**, 33–38.

55 H. M. Fares and J. B. Schlenoff, *J. Am. Chem. Soc.*, 2017, **139**, 14656–14667.

56 P. Batys, S. Luukkonen and M. Sammalkorpi, *Phys. Chem. Chem. Phys.*, 2017, **19**, 24583–24593.

57 A. Michaelides, *Acta Crystallogr. Sect. A Found. Crystallogr.*, 2015, **67**, C195–C195.

58 S. T. Dubas and J. B. Schlenoff, *Langmuir*, 2001, **17**, 7725–7727.

59 M. Elzbieciak, M. Kolasinska and P. Warszynski, *Colloids Surfaces A Physicochem. Eng. Asp.*, 2008, **321**, 258–261.

60 S. T. Dubas and J. B. Schlenoff, *Macromolecules*, 2001, **34**, 3736–3740.

61 N. Parveen and M. Schönhoff, *Soft Matter*, 2017, **13**, 1988–1997.